Connecting Coronal Mass Ejections To Their Source Regions And Studying Their Kinematical Properties

NIUS Final Term Report
by
Aarushi Rawat

under the supervision of
Prof. Dipankar Banerjee and Mr. Satabwda Mazumdar

Submitted to
HBCSE,TIFR
for NIUS 16 Physics

NIUS 16 Physics
Homi Bhabha Centre for Science Education
Tata Institute of Fundamental Research
V.N. Purav Marg Mankhurd, Mumbai 400088

Certificate

This is to certify that the report for the project titled "**CONNECTING CORONAL MASS EJECTIONS TO THEIR SOURCES AND STUDYING THEIR KINEMATICAL PROPERTIES**" was prepared in fulfilment of the requirements of NIUS 16 (Physics) by **Aarushi Rawat** affl. Sri Venkateswara College, University of Delhi under the guidance of **Prof. Dipankar Banerjee** affl. ARIES, Nainital and **Mr. Satabdwa Mazumdar** affl. Indian Institude of Astrophyscis, Bengaluru.

Prof. Dipankar Banerjee
(Guide)
Director
ARIES
Nainital

Contents

Acknowledgement

I would like to express my heartfelt gratitude towards my mentor Prof. Dipankar Banerjee and Mr. Satabdwa Mazumdar. It is through their guidance and patience that has enabled me to produce this work. Needless to say, their unwavering support and belief encouraged me throughout this project.

I would also like to thank the institution, Homi Bhabha Centre for Science Education (HBCSE),TIFR for giving me the opportunity to work on this project, and Indian Institute of Astrophysics for hosting to work on this project

Finally, my deep and sincere gratitude to my family for their continuous and unparalleled love, help and support.

List of Tables

List of Figures

Chapter 1

Introduction

Coronal Mass Ejections (CMEs) are dynamic, complex events that provide valuable insights about the nature of the solar atmosphere and the sun's magnetic field. They appear as bright, white-light features moving outward in the coronagraph field of view (FOV) (Hundhausen et al, 1984; Schwenn,1996).

They are observed in visible white light by coronagraphs which block out the light from the photosphere leaving the relatively faint surrounding corona. CMEs are a key area of interest for both scientific and technological reasons. Scientifically, because they remove built-up magnetic energy and plasma from the solar corona (Low, 1996), show a wide range of kinematics like speed ranging from 100-3000 kmps and are major drivers of space weather. And technologically, because they are responsible for the extreme space weather effects on Earth (Baker et al.,2008), as well as at other planets and spacecraft throughout the heliosphere.

Chapter 2

Motivation

In order to get a better understanding about the underlying physics and kinematical properties of the CMEs and their origin, a direct correlation between CMEs and their source regions is required. This will help in getting a sense of the importance of projection effects for CMEs from the different source regions. We know that solar cycles vary from a maxima and minima of its magnetic activity and this can be seen through its sunspot number. So correlating CMEs to their source regions would also indicate whether this maxima minima cycle affects the occurrence of respective CMEs. Moreover, getting the information of latitudes and longitudes of source regions along with the polar angles of the CMEs already given in the CDAW catalogue will help in getting the complete picture of the origin of the CMEs.

Chapter 3

Aim

1. To categorize and compare the kinematical properties of CMEs along with their source regions between the decaying phase of the 23rd and 24th solar cycle.
2. To categorize and check for imprints of source regions on the statistical properties of CMEs between the maxima of 24th solar cycle and decaying phase of 23rd and 24th solar cycle.

Chapter 4

Data Used

The data used to classify CMEs according to their source regions was done using Coordinated Data Analysis Workshops (CDAW) catalogue (Yashiro et al., 2004; Gopalswamy et al., 2009) . The values of Date, Time, Position Angle, Speed and Width were used to determine the onset, location and kinematical properties of the CME. The catalogue contains data of 24 hrs a day from 1996. The speed of CMEs listed in the catalog is the linear speed of the leading edge of a CME with no acceleration assumption. The width of a CME is defined as the maximum angle subtended by a CME on the center of the Sun when the CME enters the LASCO C3 field of view where the width appears to approach a constant value. However, this work has been based on a subset of this data. The data studied is from both 23rd and 24th solar cycle for different time periods, i.e.

1. January-August 2004 (23rd Solar Cycle Decaying Phase)
2. July-December 2013 (24th Solar Cycle Maxima Phase)
3. January-December 2017 (24th Solar Cycle Decaying Phase)

Moreover, the data has been cleaned to remove "very poor" CMEs as reported by Wang and Colaninno (2014). These "very poor" CMEs may be real CMEs but because they contain large errors in measurement of their properties, they were removed. Furthermore, only CMEs lying within the limits 30° ¡ width ¡ 180° are selected for the study. This has been done as Yashiro et al. (2008) and Gopalswamy et al. (2010) have reported that on comparison between CDAW and CACTus catalogs there exists a discrepancy in the detection of the number of CMEs in case of narrow CMEs (width <30°). Along with this Yashiro et al. (2003) has also reported that narrow CMEs do not form a subset of normal CMEs and have different acceleration mechanisms. The wide CMEs (>180°) were removed because such CMEs mostly suffer from projection effects and thus the width estimation will be affected.

ESA JHelioViewer software has been used for observational analysis and used to connect CMEs to their source regions on the solar disc.

- CMEs are observed using white light images from
    1. LASCO C2 onboard SOHO and
    2. SECCHI COR1 and COR2 onboard STEREO A and B.
- Active regions(ARs) are observed using images from
    1. Extreme Ultraviolet Imaging Telescope (EIT 195 A°) onboard SOHO,
    2. Atmospheric Imaging Assembly (AIA 171 A°, 193 A°) onboard Solar Dynamics Observatory(SDO), and also
    3. Extreme Ultraviolet Imager (EUVI 171 A°, 195 A°) onboard STEREO SECCHI A and B.
- Prominence Eruptions (PEs) are observed using images from
    1. EIT 304 A°,
    2. AIA 304 A° and
    3. EUVI 304 A°

Where the ARs, AP and PEs are defined as,

4.1 Active Regions (ARs)

These are areas of strong magnetic field, predominantly hotter and denser than the background coronal plasma, producing bright emission in the soft X-ray and extreme ultraviolet regions.

4.2 Prominence Eruptions (PEs)

are cool dense material (8000 K) embedded in the hotter corona (Gilbert et al. 2000). We detect a PE if we get to see a strong radial component of motion away from the solar surface where all or some of the prominence material is seen to escape the gravitational field of the Sun. For a filament eruption (included in the same category with PEs) we either looked for tangential motion across the solar surface with a subsequent eruption, or simply by observing any disappearance of the filament in the subsequent images with a transient coronal manifestation following it (Webb and Hundhausen, 1987).

4.3 Active Prominences (APs)

are quite prominences whose foot points are connected to Active Regions.

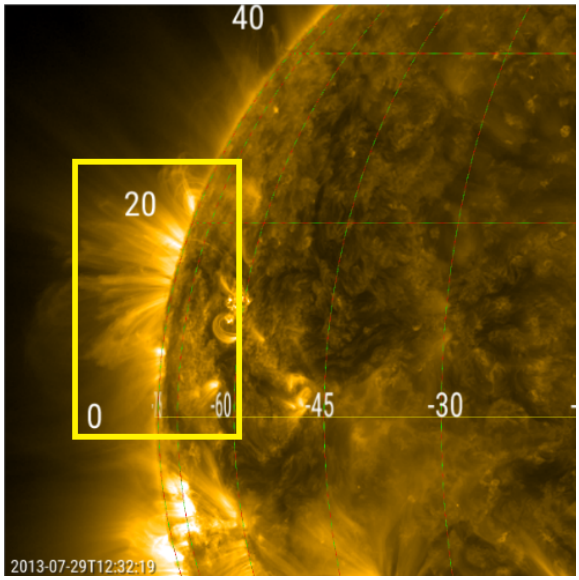

(a) Image from AIA 171 A showing the presence of an AR at the footprint of the AP

Figure 4.1: Images depicting the three souce regions of a CME

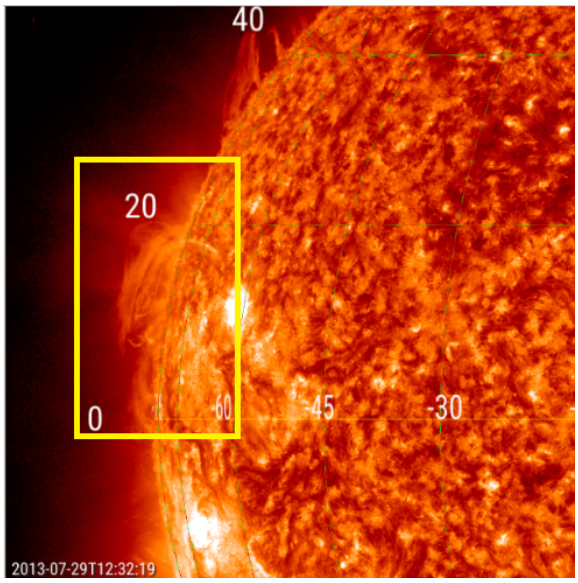

(a) image from AIA 304 A showing a AP

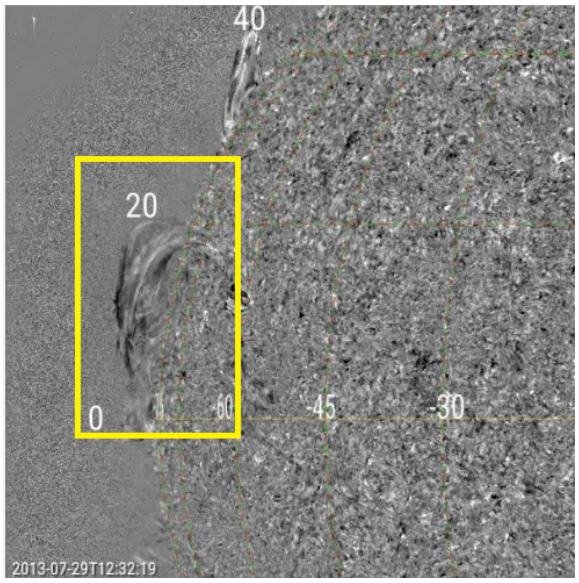

(b) running difference image of same AP

Chapter 5

Working Methodology

1. CMEs recorded in the CDAW catalogue with their dates and time were taken one by one and entered into the software.
2. Then the necessary images were loaded from AIA 304 A°, 171 A°, LASCO C2, STEREO SECCHI etc.
3. Polar Angle of the CMEs from the CDAW catalogue was used to get an idea about the probable location of the source region.
4. For a spatial association between an activity in the source region and a subsequent CME, the latitude of the source region was taken to be around 30° to that of the Position Angle (PA) of the center of CME as reported in the CDAW catalogue.
5. For the Temporal Association, the speed of the CMEs given in CDAW catalogue was noted to estimate the time range within which the source regions had to be found.
6. On locating a source region, its latitude and longitude were noted down.
    - Coordinates for ARs were taken to be at the center of the flaring region.
    - For PEs, the mean of coordinates of both the foot points was estimated and recorded.
    - For APs, the coordinates of the AR on which one leg of the eruption sits was recorded.

Chapter 6

Results And Discussion

The distribution of source regions obtained are given in the table below-

	Total	Active Region	Active Prominence	Prominence Eruption	NDA#	Blanks*
2004	397	148	42	34	70	103
2013	914	507	158	195	54	0
2017	279	211	21	13	20	14

No data available for these events on Jhelioviewer servers

* Backside events (from SOHO line of sight) which could not be recorded due to absence/unavailability of STEREO A/B data

Table 6.1: Distribution of source regions of CMEs

6.1 Comparing Decaying Phase of 23rd solar cycle (2004) and Decaying Phase of 24th solar cycle (2017)

6.1.1 Latitude Vs Position Angle (2004 vs 2017)

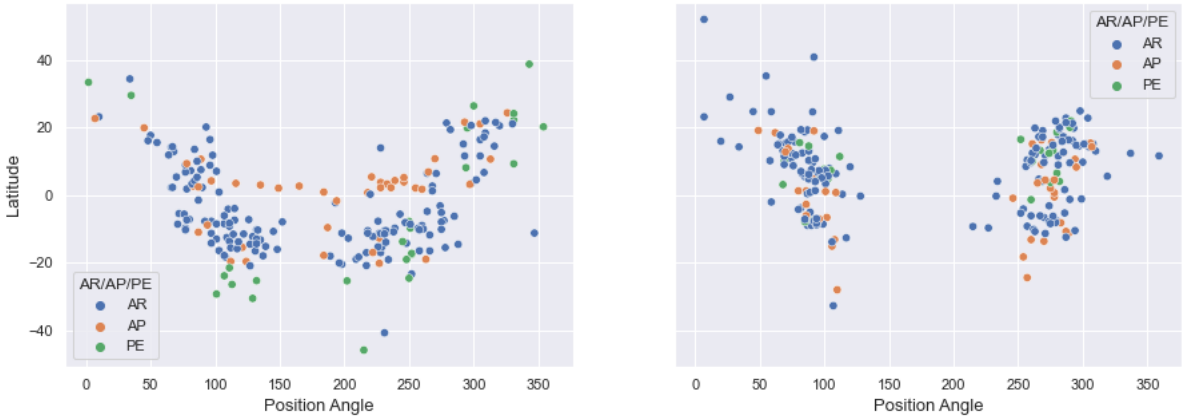

Figure 6.1: Latitude Vs Position Angle

Studying the Latitude Vs Position Angle scatter plot, some interesting points can be observed. The APs and ARs in 2004 are mostly concentrated between± 20° latitude and have a concave up "U" shaped spread. In contrast to this, in 2017 ARs are slightly spread beyond ± 20°latitude and do not have a trend to their spread. This can however be explained due to absence of any CME in between +128° to +176° in the CDAW catalog in 2017. PEs in both cases fail to show a complete curve however it could be visible once more data points are included. Therefore due to a small sample set, we can't see very conclusive features.

6.1.2 Latitude Distribution (2004 vs 2017)

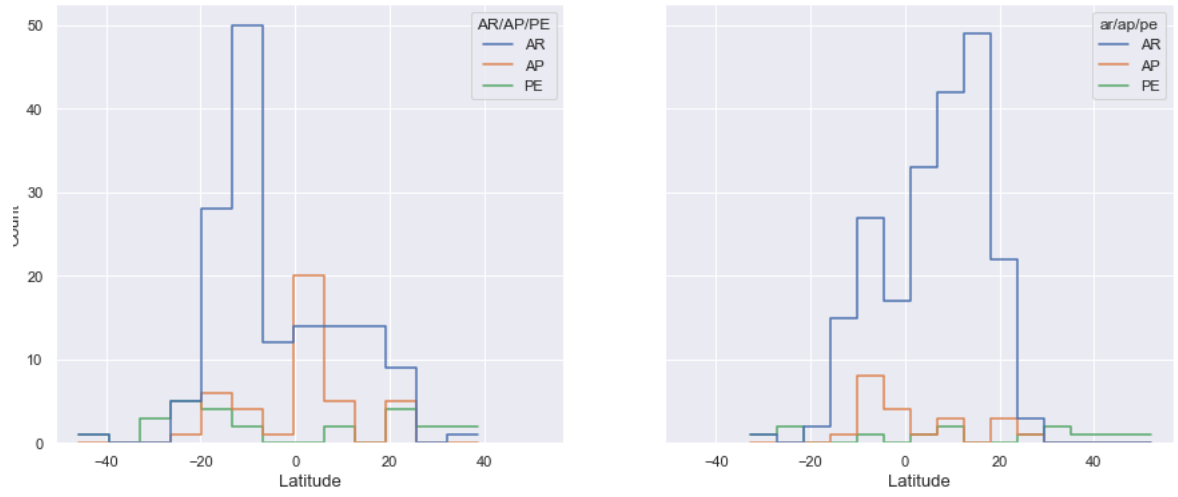

Figure 6.2: Latitude Distribution

The Latitude distribution in both cases depict a bimodal distribution for ARs, however it can be noticed that ARs had a southern hemisphere preference in 2004 (23rd solar cycle) and a northern hemisphere preference 2017 (24th solar cycle). Interestingly, APs show an opposite trend of northern hemisphere

preference in 2004 and southern hemisphere preference in 2017. This distinction however is not evident in PA distribution which points to the fact that PA is a quantity that largely suffers from projection effects and thus conclusions drawn from it can be misleading. Due to a small sample set, the distribution of PEs is not clearly visible but has a more even distribution than other source regions.

6.1.3 Position Angle Distribution (2004 vs 2017)

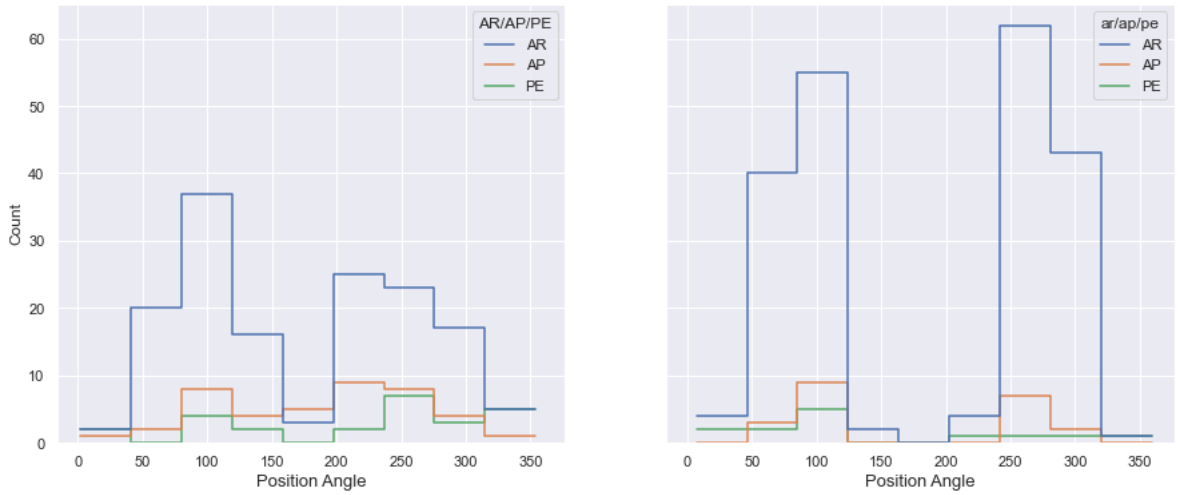

Figure 6.3: Position Angle Distribution

The PA distribution is also bimodal for both ARs and APs. Here the trend of peaks is also opposite, where 2004 has a preference towards +90°PA (westward from sun-earth line of sight) and 2017 has a preference towards +270° (eastwards from the sun-earth line of sight). Another thing to notice is the spread of peaks is more in 2004 indicating CMEs originated from a much more

dispersed area. The PEs again show slightly bimodal peaks in 2004 and mostly even spread in 2017, however this ambiguity can be resolved once more data from the decaying phase of the solar cycles is studied.

6.1.4 Speed and Width Distribution (2004 vs 2017)

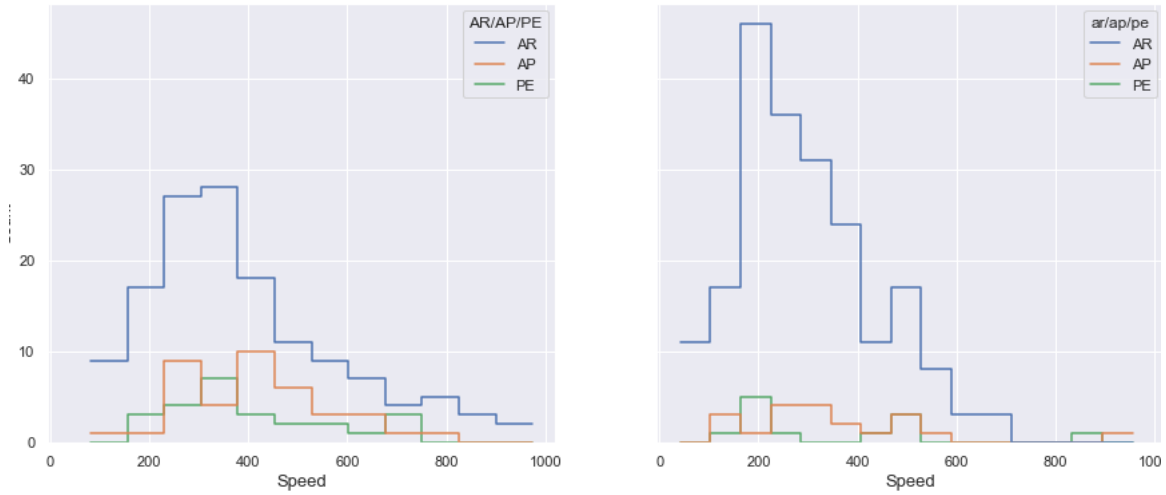

Figure 6.4: Speed Distribution

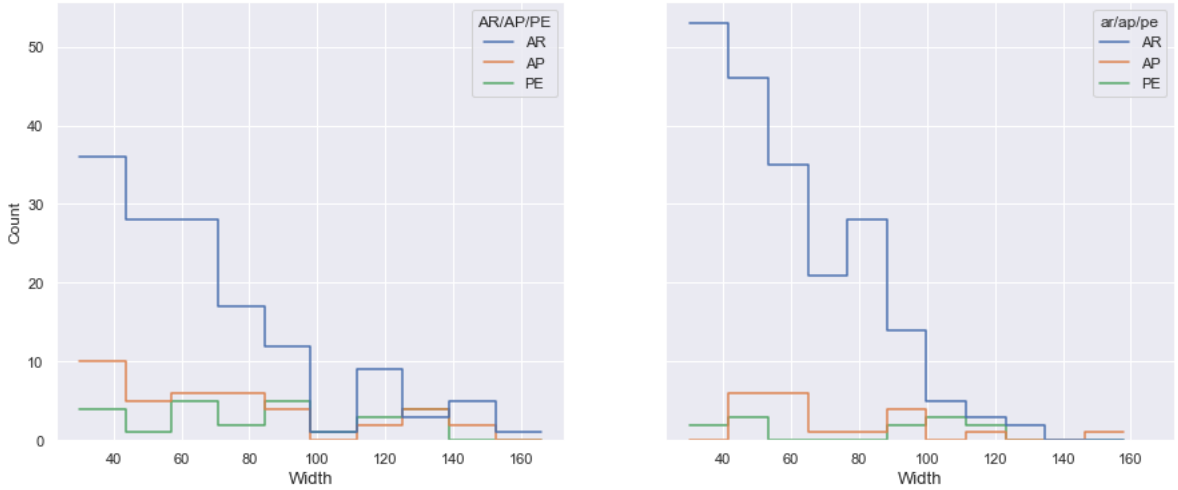

Figure 6.5: Width Distribution

The speed and width distribution of ARs for both years show a decaying trend as the values increase. The speed distribution shows a gaussian distribution whereas the width distribution power law type distribution whose implications can be drawn from Pant et al. 2021. The trend for APs and PEs is however relatively even and ambiguous due to their sample set. It can be noted that majority CMEs in both cases are slow and narrower.

6.1.5 Speed vs Width (2014 vs 2017)

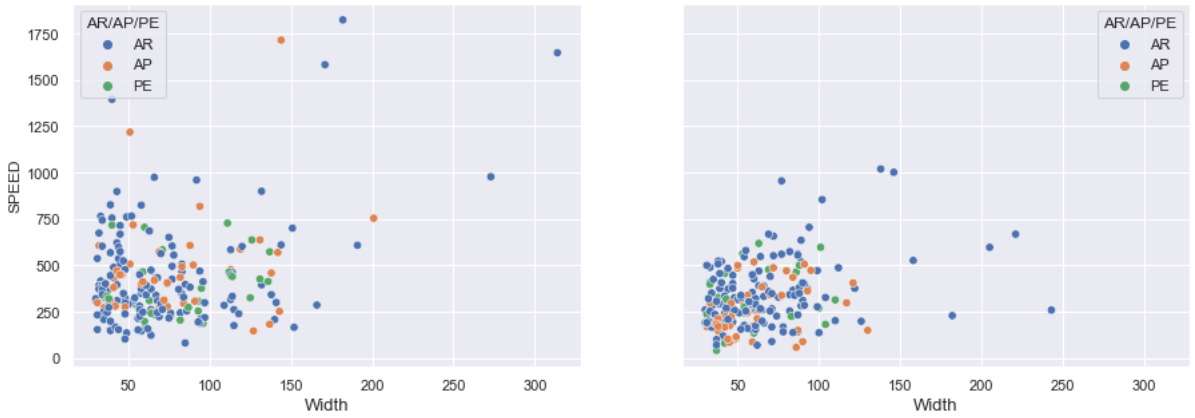

Figure 6.6: Speed vs Width

The Speed vs Width Scatter Plot suggests there is a positive correlation between them, which means that greater the speed of a CME, more will be its width. However, fitting a regression line and obtaining correlation coefficients came ¡1, however it was greater for 2017 which has more data points. Since the number of events considered is too less to come up with a strong correlation coefficient and a regression relation, this can be achieved in future with better statistics.

6.2 Comparing Maxima (24th solar cycle) and Decaying Phase (23rd and 24th solar cycle)

6.2.1 Latitude Vs Position Angle (Maxima vs Decaying Phase)

Figure 6.7: Latitude Vs Position Angle

The Latitude vs PA Scatter Plot shows interesting features for both the phases. Due to the presence of sufficient data in 2013 solar maxima phase, we can see clear features of its graph. The AR and APs are concentrated within ±20° latitude whereas PE is spread throughout the range. The ARs and APs show a concave up "U" shaped curve which arises due to the relation between the latitude and PA. There is however a deviation from this trend in case of PEs which is concave up "V" shaped curve that indicates a possible deflection in CMEs that originate from PEs. However this isn't a conclusive proof for deflection

and further analysis is required to be done in terms of unprotected latitude and longitude. In case of the decaying phase, the curves are much less defined or look incomplete due to scarcity of any CMEs present in between the 150°and 200°PA.

6.2.2 Latitude Distribution (Maxima vs Decaying Phase)

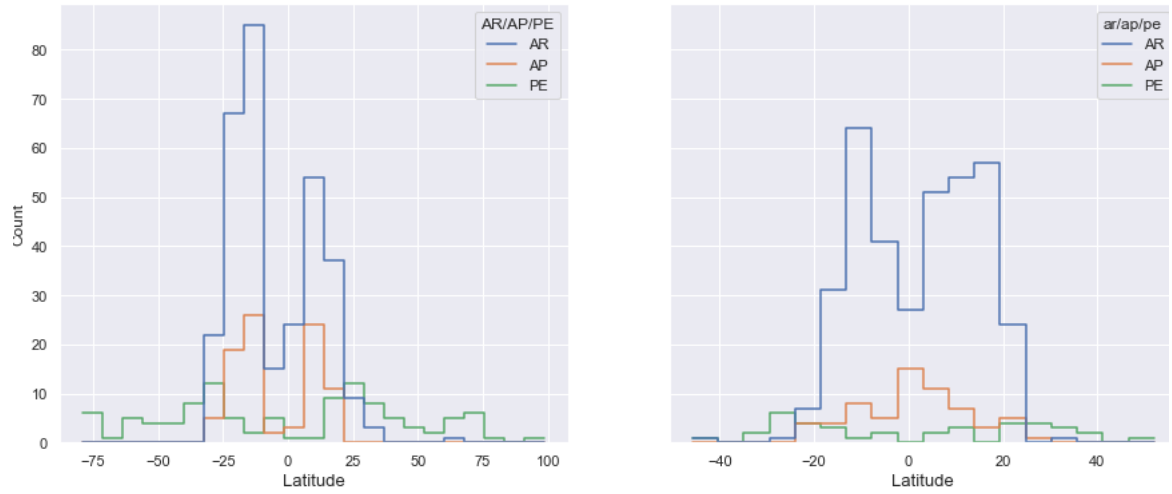

Figure 6.8: Latitude Distribution

The Latitude distribution in both cases depicts a bimodal distribution for ARs with a southern hemisphere preference. APs show a similar trend but less defined due to small numbers. PEs show an even distribution of latitude distribution for both phases.

6.2.3 Position Angle Distribution (Maxima vs Decaying Phase)

Figure 6.9: Position Angle Distribution

The PA distribution is also bimodal for both ARs and APs. Here as well we can see a slight westward preference. It can also be observed that there is almost an absence of source regions near the equator for the maxima phase whereas the decaying phase shows a significant number of source regions near the equator. PEs again show an even distribution of PA for both phases. The PA distribution for both

phases show broader peaks than their corresponding latitude distribution which is quite narrow, this could be because of drifting or deflection of CMEs after they erupt from the surface and spread out in the corona.

6.2.4 Speed and Width Distribution (Maxima vs Decaying Phase)

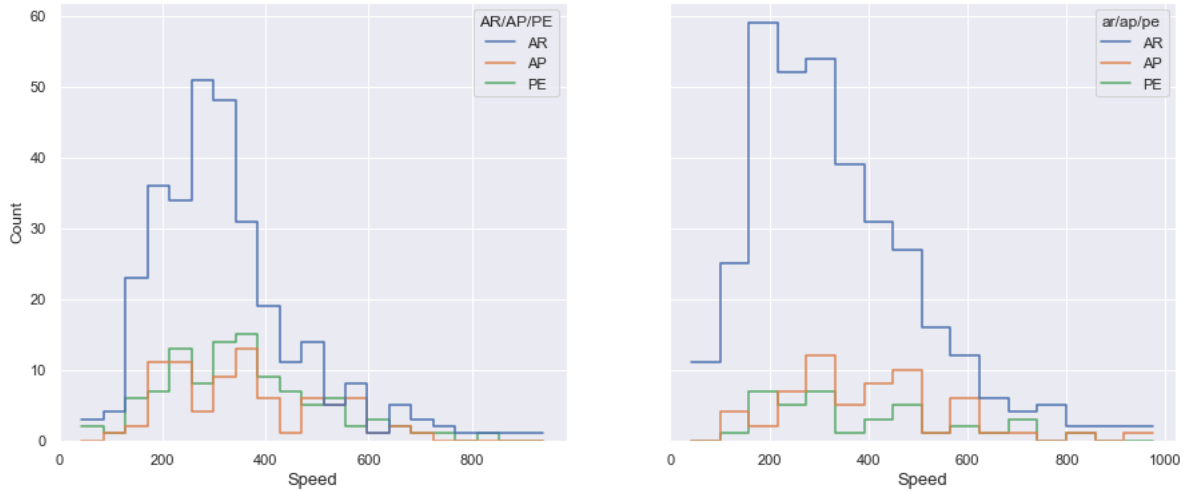

Figure 6.10: Speed and Width Distribution

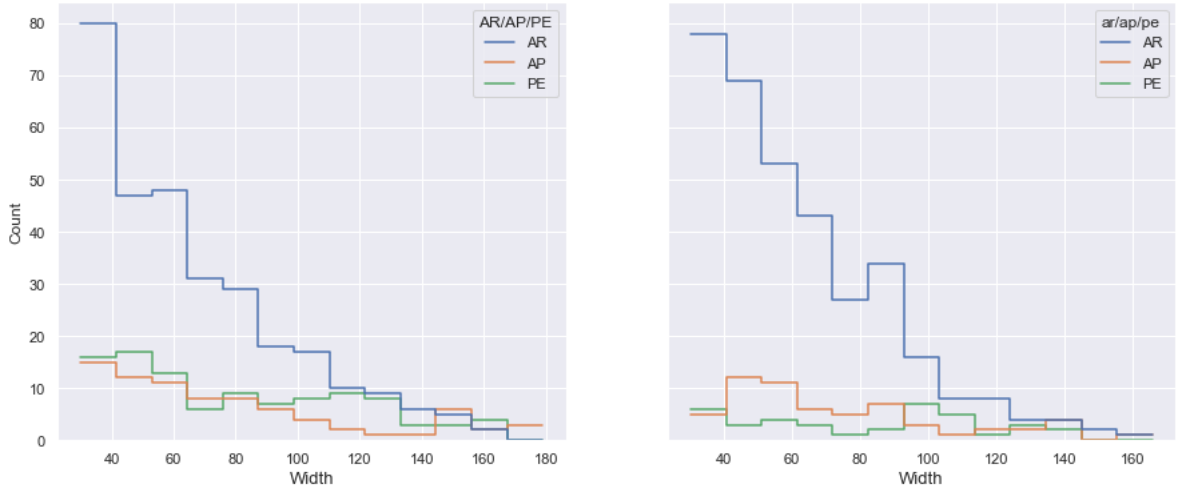

Figure 6.11: Speed and Width Distribution

The speed and width distribution of ARs for both years show a decaying trend as the values increase. The decay in speed and width for both speed and width distribution seems steeper for the maxima phase however a power law must be fitted to get accurate comparisons. It can again be noted that majority CMEs in both cases are slower and narrower.

6.2.5 Speed vs Width (Maxima vs Decaying Phase)

Figure 6.12: Speed vs Width

The Speed vs Width Scatter Plot suggests there is a positive correlation between them, which means that greater the speed of a CME, more will be its width. However, fitting a regression line and obtaining correlation coefficients came out as r0.35 for maxima phase and r0.15 for the decaying phase which shows a poor correlation between the two.

Chapter 7

Conclusion

This has helped in gaining several interesting insights into CME propagation and their kinematical properties which are summarised below. From the graphical comparison between the Decaying Phase of 23rd solar cycle (2004) and Decaying Phase of 24th solar cycle (2017), it could be seen from the Latitude Vs Position Angle scatter plot that 2017 had a slightly more spread of latitude ARs than 2004 suggesting more magnetic activity throughout the sun's surface during the decaying phase of 2017. The Latitude distribution showed a southern hemisphere preference in 2004 (23rd solar cycle) and a northern hemisphere preference 2017 (24th solar cycle). And interestingly APs show an opposite trend of northern hemisphere preference in 2004 and southern hemisphere preference in 2017. The PA distribution showed same opposite trend, where 2004 has a preference towards +90°PA (westward from sun-earth line of sight) and 2017 has a preference towards +270°(eastwards from the sun-earth line of sight). Another thing to notice is the spread of peaks is more in 2004 indicating CMEs originated from a much more dispersed area. The Speed vs Width Scatter Plot depicted a positive correlation between them. The speed and width distribution of ARs for both years showed a decaying trend as the values increase and majority CMEs in both cases are slow and narrow.

On comparing Maxima Phase of 24th solar cycle (2013) and combined Decaying Phase of 23rd and 24th solar cycle (2004 and 2017), it could be seen that the PA Distribution shows ARs and APs with a concave up "U" shaped curve which arises due to the relation between the latitude and PA. PEs showed a deviation from this trend with a concave up "V" shaped curve that indicates a possible deflection in CMEs that originate from PEs. The Latitude distribution in both cases depicts a bimodal distribution for ARs with a southern hemisphere preference. The PA distribution is also bimodal for both ARs and APs with a slight westward preference. It was also observed that there is almost an absence of source regions near the equator for the maxima phase whereas the decaying phase shows a significant number of source regions near the equator. The PA distribution for both phases show broader peaks than their corresponding latitude distribution which is quite narrow, this could be because of drifting or deflection of CMEs after they erupt from the surface and spread out in the corona. The speed and width distribution of ARs for both years show a decaying trend as the values increase. The decay in speed and width for both speed and width distribution seems steeper for the maxima phase however a power law must be fitted to get accurate comparisons. It can again be noted that majority CMEs in both cases are slower and narrower. The Speed vs Width Scatter Plot suggests there is a positive but poor correlation between them.

Chapter 8

Future Prospects

Although there is still a lot to be uncovered and understood about CMEs from this study itself and even more from subsequent studies. Initial progress from this work can be made in increasing the data sample substantially to obtain better statistics and get finer inferences. This study can also be extended by incorporating more solar cycles and different phases of those solar cycles in order to get a complete picture of how the source regions affect the kinematics of CMEs.

Chapter 9

Bibliography

Baker, D. and Kanekal, S., 2008. Solar cycle changes, geomagnetic variations, and energetic particle properties in the inner magnetosphere. Journal of Atmospheric and Solar-Terrestrial Physics, 70(2-4), pp.195-206.

Gopalswamy, N., Yashiro, S., Michalek, G., Stenborg, G., Vourlidas, A., Freeland, S. and Howard, R., 2009. The SOHO/LASCO CME Catalog. Earth, Moon, and Planets, 104(1-4), pp.295-313.

Hundhausen, A., Sawyer, C., House, L., Illing, R. and Wagner, W., 1984. Coronal mass ejections observed during the Solar Maximum Mission: Latitude distribution and rate of occurrence. Journal of Geophysical Research, 89(A5), p.2639.

Low, B., 1996. Solar activity and the corona. Solar Physics, 167(1-2), pp.217-265.

Schwenn, R., 1996. An Essay on Terminology, Myths, - and Known Facts: Solar Transient - Flare - CME - Driver Gas - Piston - BDE - Magnetic Cloud - Shock Wave - Geomagnetic Storm. International Astronomical Union Colloquium, 154, pp.187-193.

Wang, Y. and Colaninno, R., 2014. IS SOLAR CYCLE 24 PRODUCING MORE CORONAL MASS EJECTIONS THAN CYCLE 23?. The Astrophysical Journal, 784(2), p.L27.

Webb, D. and Hundhausen, A., 1987. Activity associated with the solar origin of coronal mass ejections. Solar Physics, 108(2), pp.383-401.

Yashiro, S., 2004. A catalog of white light coronal mass ejections observed by the SOHO spacecraft. Journal of Geophysical Research, 109(A7).

Yashiro, S., Gopalswamy, N., Michalek, G. and Howard, R., 2003. Properties of narrow coronal masse-jections observed with LASCO. Advances in Space Research, 32(12), pp.2631-2635.